
National Aeronautics and Space Administration

Compton Gamma Ray Observatory

FINAL TECHNICAL REPORT FOR NAG5-2051

*17MIL
10-89-12
0517
027734*

Submitted to: Dr. Jay P. Norris, Code 668.1
Lab for High Energy Astrophysics
NASA/Goddard Space Flight Center
Greenbelt, MD 20771

Submitted by: The Trustees of Columbia University
in the City of New York
351 Eng. Terrace
New York, New York 10027

Prepared by: Columbia Astrophysics Laboratory
Departments of Astronomy and Physics
Columbia University
550 West 120th Street, MC-5247
New York, New York 10027

Principal Investigator: Jules P. Halpern

Title of Research: "Timing the Geminga Pulsar with High-Energy
Gamma-Rays"

Termination Date: 14 February 1997

May 1997

TABLE OF CONTENTS

Summary	2
Papers Published Under NASA Grant NAG 5-2051	2
Timing the Geminga Pulsar with Gamma-Ray Observations	3

SUMMARY

This is a continuing program to extend and refine the ephemeris of the Geminga pulsar with annual observations for the remaining lifetime of EGRET. An paper incorporating all of the EGRET data on Geminga through 1997 has been submitted to *The Astrophysical Journal*, and appears as an Appendix to this report (Mattox, Halpern, & Caraveo 1997). An earlier analysis using the first 3.9 years of EGRET data appeared in a paper by Mattox, Halpern, & Caraveo (1996).

These data show that every revolution of Geminga is accounted for during the EGRET epoch, and that a coherent timing solution linking the phase between EGRET, *COS-B*, and *SAS-2*, observations has now been achieved. The accuracy of the gamma-ray timing is such that the proper motion of the pulsar can now be detected, consistent with the optical determination. The measured braking index over the 24.2 yr baseline is 17 ± 1 . Further observation is required to ascertain whether this very large braking index truly represents the energy loss mechanism, perhaps related to the theory in which Geminga is near its γ -ray death line, or whether it is a manifestation of timing noise. Statistically significant timing residuals are detected in the EGRET data; they depart from the cubic ephemeris at a level of 23 milliperiods. The residuals appear to have a sinusoidal modulation with a period of about 5.1 yr. This could simply be a manifestation of timing noise, or it could be consistent with a planet of mass $1.7/\sin i M_{\oplus}$ orbiting Geminga at a radius of $3.3/\sin i$ AU.

Papers Published Under NASA Grant NAG 5-2051

“Timing the Geminga Pulsar with EGRET Data,” J. R. Mattox, J. P. Halpern, & P. A. Caraveo *Astr. Ap. Suppl.*, **120**, C77 (1996).

“Timing the Geminga Pulsar with Gamma-ray Observations,” J. R. Mattox, J. P. Halpern, & P. A. Caraveo *Ap. J.*, submitted (1997).

Timing the Geminga Pulsar with Gamma-Ray Observations

J. R. Mattox ¹, J. P. Halpern ², and P. A. Caraveo ³

ABSTRACT

We present the “*COS-B/EGRET 97*” ephemeris for the rotation of the Geminga pulsar. This ephemeris uses the accurate position and proper motion recently obtained by Caraveo et al. (1997). A cubic ephemeris predicts the rotational phase of Geminga with errors smaller than 50 milliperiods for all existing high-energy γ -ray observations that span a 24.2 yr timing baseline. The braking index obtained is 17 ± 1 . Further observation is required to ascertain whether this high value truly reflects the energy loss mechanism, or whether it is a manifestation of timing noise. The ephemeris parameters are sufficiently constrained so that timing noise will be the limitation on forward extrapolation. If Geminga continues to rotate without a glitch as it has for the past 24 yr, we expect this ephemeris to continue to describe the phase with an error less than 100 milliperiods until the year 2008. Statistically significant timing residuals are detected in the EGRET data; they depart from the cubic ephemeris at a level of 23 milliperiods. Although this could simply be an additional manifestation of timing noise, the EGRET timing residuals appear to have a sinusoidal modulation that is consistent with a planet of mass $1.7/\sin i M_{\oplus}$ orbiting Geminga at a radius of $3.3/\sin i$ AU.

1. Introduction

The isolated pulsar “Geminga” is the second brightest high-energy γ -ray source in the sky (Thompson et al. 1977, Bennett et al. 1977, Bertsch et al. 1992), but it has a small radio flux if any (Kuzmin & Losovsky 1997; Malofeev & Malov 1997). Therefore, high-energy observations are currently the principal means to time the rotation of Geminga. The *ROSAT* detection of periodic X-ray emission (Halpern & Holt 1992) with a period of 237 ms lead to a successful search for periodicity in the nearly contemporaneous EGRET data (Bertsch et al. 1992), as well as in the archival *COS-B* (Bignami & Caraveo 1992, Hermesen et al. 1992) and *SAS-2* data (Mattox et al. 1992). This established that Geminga is a rotation-powered pulsar with surface magnetic field $B_p \sim 1.6 \times 10^{12}$ G and spin-down age $\tau = P/2\dot{P} = 3.4 \times 10^5$ yr. Preliminary analyses of the EGRET data were presented by Mayer-Hasselwander et al. (1994) and Fierro et al. (1997). *ASCA* and *EUVE* results were presented by Halpern, Martin, & Marshall (1996) and Halpern & Wang (1997). Caraveo et al. (1996) reported the detection with HST of a parallactic displacement of the optical counterpart of $0''.0064 \pm 0''.0017$ which implies a distance of 157^{+59}_{-34} pc. Caraveo et al. (1997) also obtained a position for the optical counterpart of Geminga which is accurate to ~ 40 mas by using the Hipparcos data to locate field stars in the *HST* Geminga images. A review of Geminga was published by Bignami & Caraveo (1996).

Although the periodicity of Geminga was initially found in *ROSAT* X-ray data, much more precise timing can be done with EGRET because the *ROSAT* exposures are short, the soft X-ray peaks are broad,

¹Astronomy Department, Boston University, 725 Commonwealth Ave., Boston, MA 02215

²Department of Astronomy, Columbia University, 550 West 120th Street, New York, NY 10027, USA

³Istituto di Fisica Cosmica del CNR, Via Bassini, 15, 20133 Milano, Italy

and their modulation is shallow. An ephemeris for the rotation of Geminga based on EGRET observations spanning 2.1 yr was published by Mattox et al. (1994). Subsequently, an ephemeris for observations spanning 3.9 yr was presented (Mattox, Halpern, & Caraveo 1996). New observations now extend the baseline of EGRET observations to 5.9 yr. This long baseline allows the rotation parameters of Geminga to be sufficiently constrained so that the rotation phase during EGRET observations can be compared to the phase during *COS-B* observations. We thus obtain a cubic ephemeris that describes the rotation of Geminga from the beginning of *SAS-2* observations (1973.0) to the end of the most recent EGRET observation (1997.2) with timing residuals that are less than 50 milliperiods. The fact that these residuals are small implies that Geminga has not glitched during the past 24 yr, and that we can count all 1.2 billion rotations of Geminga between the last *COS-B* observation (1982.3) and the first EGRET observation (1991.3) even though they were not observed. With the second derivative of frequency tightly constrained by this long baseline, significant timing residuals have become apparent.

2. The Derivation of a Cubic Ephemeris from the *SAS-2*, *COS-B*, and EGRET Observations

As described by Mattox et al. (1994, 1996), the ephemeris parameters are estimated as the values which give the largest value of the Z_{10}^2 statistic (i.e., the most non-uniform light curve). We seek a simple representation of the time dependence of the phase of Geminga. The first three terms of a Taylor's series form a cubic ephemeris:

$$\phi = \phi_0 + f(t - t_0) + \dot{f}(t - t_0)^2/2 + \ddot{f}(t - t_0)^3/6 \quad (1)$$

where t_0 is the epoch, and t is time at the solar system barycenter. Error in the position used when correcting photon arrival times to the barycenter can cause error in the derived ephemeris parameters (e.g., Bisnovatyi-Kogan & Postnov 1993). Mattox et al. (1996) show that the maximum possible error in corrected arrival time is $2.3\delta_e$ ms where δ_e is the position error in arcsec. With the ability to resolve phase to ~ 5 milliperiods with γ -ray observations to date, errors in the position of Geminga larger than $0''.5$ will affect the timing solution. The recent determination of the time dependent position of Geminga to within ~ 40 mas (Caraveo et al. 1997) is an order of magnitude better than required for this. The position at the epoch of the *HST* observation and the proper motion as given in Table 1 are assumed for our analysis.

In order to compare the rotational phase of Geminga during the *COS-B* observations to the EGRET phase, we have updated the *COS-B* barycenter. This was necessary because the MIT PEP 740 ephemeris for the solar system that the *COS-B* team used yields a barycenter position that is a substantial distance from the barycenter position obtained with the JPL DE 200 solar system ephemeris that the EGRET team uses. This discrepancy results from updated values for the masses of the outer planets obtained recently through spacecraft fly-by. The update for the *COS-B* data was not simple because the position of the *COS-B* spacecraft for each event is not available in modern databases. Rather than attempt to resurrect and reanalyze a large number of old magnetic tapes, we have used the MIT PEP 740 ephemeris to recover the *COS-B* spacecraft position from the old barycenter direction vector for each *COS-B* event. These positions were observed to be consistent with the *COS-B* orbit. The spacecraft position for each *COS-B* event was then used with the JPL planetary ephemeris to obtain a new barycenter direction vector for each event.

We initially analyzed the EGRET data alone. With the new observations (viewing periods 419.1, 419.5, 420, 426, 502, 510, 510.5, 526, 527, 528, & 616.1), the EGRET observations now span 5.9 yr. We previously analyzed EGRET events selected with energy $E > 70$ MeV (Mattox et al. 1994, 1996). However, an

investigation of the potential for resolving rotation phase with EGRET data described below led to a new energy selection for this work, $E > 100$ MeV. No loss in timing accuracy is observed to result. In addition, variation in the shape of the light curve with the spectral response of EGRET as the spark-chamber gas ages, and the consequent impact on phase measurement, is reduced with this selection. Events were selected from an energy-dependent cone encompassing 68% of the point spread function at each energy. To eliminate contamination from Earth albedo γ -rays, the minimum accepted angle from the horizon was an energy-dependent 4σ cut based on the EGRET PSF.

The downhill simplex method (Press et al. 1992) was used to simultaneously estimate the f and \dot{f} which produced a maximum Z_{10}^2 statistic for various \ddot{f} . This search only finds local maxima. Previous grid searches (as described by Mattox et al. 1994, 1996) allow us to begin the downhill simplex search near a global maximum. We then confirm that a result is the global maximum by examining the timing residual for each observation as described below.

The cubic ephemeris thus obtained for EGRET with $T_0 = \text{JD } 2448750.5$ is: $f = 4.21766909394(3)$, $\dot{f} = -1.95226(1) \times 10^{-13}$, and $\ddot{f} = 8.0(8) \times 10^{-25}$. The uncertainty of the last digit of each parameter is indicated by the digit in parenthesis. This corresponds to a decrease by 5.1 in the Z_{10}^2 statistic corresponding to a bootstrap determination of the 95% confidence interval (Mattox et al. 1994). A full analysis of covariance has not been done. However, in determining the uncertainty of \ddot{f} , both f and \dot{f} were optimized for each value of \ddot{f} considered. Likewise, in determining the uncertainty of \dot{f} , f was optimized for each value of \ddot{f} considered. The corresponding braking index, $\eta = f\ddot{f}/\dot{f}^2 = 89 \pm 9$, is much higher than the value of $\eta = 3$ expected for magnetic dipole radiation. This discrepancy is discussed below.

The same analysis for the COS-B data alone with $T_0 = \text{JD } 2443946.5$ yields: $f = 4.2177501227(1)$, $\dot{f} = -1.95239(2) \times 10^{-13}$, and $\ddot{f} = 4.5(2.0) \times 10^{-25}$. This value of \ddot{f} is consistent with that of Hermsen et al. (1992). Because the accurate position and proper motion of Caraveo et al. (1997) were used for this analysis, we can reject the hypothesis of Bisnovatyi-Kogan & Postnov (1993) that the large value of \ddot{f} reported by Hermsen et al. (1992) is due to proper motion. Another explanation is proposed in §4.

We note that the COS-B and EGRET values for \ddot{f} are inconsistent. Furthermore, the value obtained from the two measurements of \dot{f} ,

$$\ddot{f} = \frac{\dot{f}_{\text{EGRET}} - \dot{f}_{\text{COS-B}}}{T_{0\text{EGRET}} - T_{0\text{COS-B}}} = 3.1(5) \times 10^{-26}, \quad (2)$$

although consistent with a braking index of 3, is not consistent with either the COS-B value for \ddot{f} nor with the EGRET value. These discrepancies can be attributed to timing noise. However, they make the search for a timing solution which would coherently connect COS-B and EGRET problematic. Notwithstanding, having coherent solutions for 6.7 yr of COS-B data and 5.9 yr of EGRET data, it seemed plausible to find a coherent solution which would bridge the 9.0 yr gap between these observations.

In the search for a coherent COS-B/EGRET timing solution, the downhill simplex method was used to estimate f , \dot{f} , and \ddot{f} . The search was initiated at ≈ 1000 different initial values of these three parameters to attempt to find a global maximum in the midst of hundreds of local maxima. After several days of processing, a solution which gave a relatively large value for Z_{10}^2 was found. The cubic ephemeris thus obtained for COS-B/EGRET with $T_0 = \text{JD } 2446600$ is:

$$\begin{aligned} f &= 4.217705363090(13) \\ \dot{f} &= -1.9521717(12) \times 10^{-13} \\ \ddot{f} &= 1.48(3) \times 10^{-25} \end{aligned} \quad (3)$$

Unlike the local maxima, equation 3 produces a light curve for all observations which, except for variable instrument response and statistical fluctuation, was found through visual inspection to be consistent with an invariant shape and phase. A detailed analysis of timing residuals follows. We also found that the *SAS-2* Geminga data (Mattox et al. 1992) yielded the same phase using equation 3. The light curve obtained with equation 3 for the EGRET data is nearly identical to that of Figure 1. The braking index implied by equation 3 is 17 ± 1 . We discuss in §4 the discrepancy with the value of 3 expected if magnetic dipole radiation is the dominant energy loss mechanism.

It is of interest to compare the uncertainties of the parameters in equation 3 with expectation. A rough estimate of the expected resolution of each term in a cubic ephemeris is:

$$\delta f \approx \frac{q}{\Delta T} = 1.5 \times 10^{-11} \text{ Hz} \quad (4)$$

$$\delta \dot{f} \approx \frac{2q}{\Delta T^2} = 4. \times 10^{-20} \text{ Hz s}^{-1} \quad (5)$$

$$\delta \ddot{f} \approx \frac{6q}{\Delta T^3} = 2. \times 10^{-28} \text{ Hz s}^{-2} \quad (6)$$

where q is the phase resolution typical of a γ -ray observation, $q \sim 0.01$, and $\Delta T = 21.6$ yr time from the first *COS-B* observation to the last EGRET one. The resolution of f found in equation 3 slightly exceeds this expectation. The resolution of \dot{f} in practice is a factor of 3 worse, and the resolution of \ddot{f} a factor of 15 worse. This reflects the fact that the higher order terms cause rapid phase variation far from the epoch and the phase resolution is therefore worse because it must be obtained with a small fraction of the exposure. As expected, the discrepancy is more pronounced for the cubic term than for the quadratic term.

We note in passing that the transverse velocity of Geminga, $v_t = 122 \text{ km s}^{-1}$, causes the observed \dot{f} to be larger than the intrinsic value, \dot{f}_i , by the kinematic contribution, $\dot{f}_k = \dot{f}_i v_t^2 / cD$ (Shklovskii 1970), where D is the distance to the pulsar. For Geminga this is not an important effect, $\dot{f}_k / \dot{f}_i = 2 \times 10^{-4}$, because \dot{f}_i is relatively large.

3. Analysis of Gamma-Ray Timing Residuals

With abundant Geminga events from a deep EGRET exposure, a visual inspection of the lightcurve can resolve phase to ~ 10 milliperiods. However, with the very sparse statistics of *SAS-2*, *COS-B*, and weak EGRET exposures, it is not feasible to assess phase accurately through a visual inspection. Therefore, a means to quantitatively assess γ -ray phase has been developed.

This analysis is made more difficult by the dramatic changes of the spectrum of the γ -ray emission with the phase of Geminga (Mayer-Hasselwander et al. 1994, Fierro et al. 1997). The different spectral responses and background levels of the three γ -ray telescopes thus result in different light curves. Also, the spectral response of each telescope becomes gradually harder as the spark-chamber gas ages, and then reverts to a softer response when the gas is replaced. Since a detailed model of the dynamic spectrum is not available (private communication, R. Romani, 1997), an empirical approach has been taken.

The lightcurve of each Geminga observation was fitted with the following *ad hoc* function:

$$\begin{aligned} F(\phi) &= F_{b2} + [F_{p2} - F_{b2}] * [1 + (\phi - \phi_2)^2 / W_{p2a}^2]^{-1}, & \phi_2 - 0.25 < \phi < \phi_2 \\ F(\phi) &= F_{b1} + [F_{p2} - F_{b1}] * [1 + (\phi - \phi_2)^2 / W_{p2b}^2]^{-1} + [F_{p1} - F_{b1}] * [1 + (\phi - \phi_1)^2 / W_{p1a}^2]^{-1}, & \phi_2 < \phi < \phi_1 \\ F(\phi) &= F_{b2} + [F_{p1} - F_{b2}] * [1 + (\phi - \phi_1)^2 / W_{p1b}^2]^{-1}, & \phi_1 < \phi < \phi_1 + 0.25 \end{aligned} \quad (7)$$

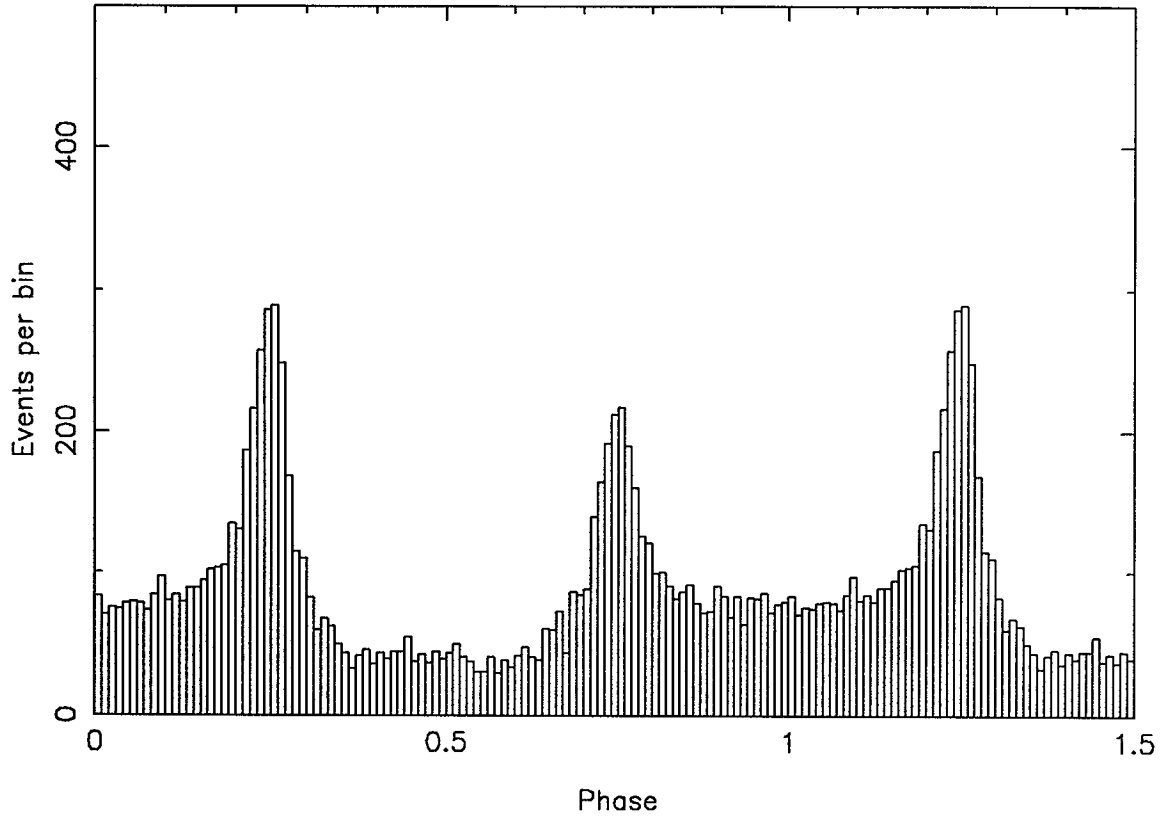


Fig. 1.— The phase dependence of the Geminga γ -rays detected by EGRET with $E > 100$ MeV as obtained with the ephemeris of Table 1. A phase offset of 0.194 has been added for the purpose of display so that peak one is at phase 0.75. Peak one precedes the strongest emission bridge, the “major bridge” interval. The “minor bridge” interval follows peak two. The histograms contain 8877 events from EGRET observations between 1991.3 and 1997.2. The events selection is described in the text.

This equation has four Lorentzian functions, one for each side of each peak. The phase of peak one is fixed relative to peak two, $\phi_1 = \phi_2 + 0.500$, as discussed below. The peak widths are fixed at values obtained from a deep EGRET exposure (the sum of VPs 0.2, 0.3, 0.4, 0.5, 1.0, & 2.5): $W_{p2a} = 0.0297$, $W_{p2b} = .0233$, $W_{p1a} = 0.0343$, $W_{p1b} = 0.0287$. Five parameters were adjusted using the downhill simplex algorithm to optimize the fit to each observation: ϕ_2 , the phase of peak two; F_{b2} , the flux level of the major bridge; F_{b1} , the flux level of the minor bridge; F_{p2} , the flux level of peak two; and F_{p1} , the flux level of peak one. A phase ambiguity of 180° is averted because $F_{b2} > F_{b1}$.

The fit was compared to binned events, and the quality of the fit was assessed by a calculation of the χ^2 statistic for the difference. The width of each phase bin was adjusted to obtain a specific number of observed events in each bin. Ten events per bin was found to work well, even for weak exposures. Larger numbers of events per bin worked as well for strong exposures. The values of χ^2 obtained were generally smaller than the number of bins minus the number of optimized parameters indicating that equation 7 is an appropriate representation of the light curve, and that variation in spectral response and background is accommodated. Figure 2a shows this fit in comparison to all EGRET events. Because five parameters are fitted, the uncertainty of the phase estimate is demarcated by the change in ϕ_2 which causes an increase in χ^2 of 5.9 (11.1) for 68% (95%) confidence (Lampton Margon and Bowyer 1976; $\int_{5.9}^{\infty} \chi_5^2 = 0.32$, $\int_{11.1}^{\infty} \chi_5^2 = 0.05$). In the future, a detailed model of the dynamic spectrum of Geminga along with information about the spectral response and background for each observation could reduce the uncertainty of the phase estimate because only one parameter, ϕ_2 , would then need to be fitted.

Initial work with the deep EGRET exposure obtained in VP 0.2–2.5 found that the the separation of the two peaks is in fact 500 ± 5 milliperiods. Each peak was analyzed using data in a phase interval of 0.5 centered around the peak. An analysis of the hardness ratio of Geminga as a function of phase (Fierro et al. 1997) finds that the hardening of each peak is approximately symmetric about the peak. Thus we can expect that our method of finding the phase of a peak is not strongly affected by the spectral response of the instrument. In fact, an analysis by this method of the all EGRET exposure through 1996.7 found that the phases of both peak 1 and peak 2 are invariant for the energy bands $150 < E < 500$ MeV, $500 < E < 30,000$ MeV, and $E > 70$ MeV. The peaks in the $70 < E < 150$ MeV energy band were both shifted by 10 milliperiods toward smaller phase. Thus, an energy selection of $E > 100$ MeV was adopted for this work. Other than the expected variation of F_{b-} and F_{p-} with instrument spectral response, no indication of time variability in the light curve was seen.

Equation 7 was used to obtain a timing residual after epoch folding with the ephemeris given in equation 3 for each observation of Geminga. The resulting residuals were nearly identical to those shown in Figure 3. Some of the EGRET viewing periods have been combined for this analysis, either to provide adequate statistics, or because they are close in time. Viewing periods 0.2–0.5, 1.0, & 2.5 which provide 39 days of exposure in a 54 day interval have thus been combined. They were also analyzed separately, and gave consistent phase. Because timing noise is not expected on this time scale, this provides reassurance that our analysis of timing residuals is correct.

Amongst the EGRET points, modulation in the timing residuals is apparent. This modulation is consistent with a sinusoid of period 5.1 yr. However, with only ≈ 1 cycle of EGRET timing, it is possible that this is simply timing noise (Cordes 1993). Assuming that these residuals are timing noise, the activity parameter of Geminga can be calculated. To compare to studies of large numbers of pulsars, values of timing residuals were obtained relative to the optimal quadratic ephemeris for the EGRET data alone ($T_0 = \text{JD } 2448750.5$, $\ddot{f} = 0$, $\dot{f} = 4.21766909351(3)$, and $\ddot{f} = -1.95179(1) \times 10^{-13}$). The RMS residual was 23 milliperiods, or 5.4 ms. For reference, the Crab pulsar residuals are expected to be 19 ms for a 5.9 yr timing

baseline (Cordes 1993). Thus the activity parameter of Geminga is $\log(5.4/19) = -0.54$. Examination of Figure II of Cordes (1993) indicates that this value is somewhat larger than expected for a pulsar with the period and period derivative of Geminga. Also, if the modulation were timing noise, quasi-sinusoidal modulation is not likely. Examination of Figure I of Cordes (1993) indicates that only $\sim 10\%$ of pulsars exhibit timing noise which could appear as sinusoidal as our residuals do. Therefore, a potential planetary explanation for the apparent modulation has been explored.

The downhill simplex method was used to find the optimal f , \dot{f} , and \ddot{f} for the combined *SAS-2*, *COS-B*, and EGRET data as various orbital parameters were tried. This lead to the planetary parameters given in Table 1 along with the corresponding cubic ephemeris (which is very similar to equation 3). An eccentricity of 0.3 yields a Z_{10}^2 statistic which is better than the Z_{10}^2 statistic obtained with $e = 0$ by 9. This improvement is not highly significant, so an eccentricity of zero is assumed. The uncertainty of each orbital parameter was obtained by noting the change which caused a decrease by ~ 5 in the Z_{10}^2 statistic, corresponding to a bootstrap determination of the 95% confidence interval (Mattox et al. 1994). The resulting ephemeris is shown in Table 1.

The timing residuals shown in Figure 3 are those obtained using the cubic ephemeris in Table 1 and excluding the sinusoidal term. The addition of the sinusoidal term then fits modulation shown in the Figure. The agreement is not bad, $\chi^2=13.7$ for 10 DOF. For the optimal cubic ephemeris (equation 3), $\chi^2=54.7$ for 13 DOF ($\chi^2=67.3$ for the cubic ephemeris of Table 1 without the planetary term). This indicates with a significance of 5×10^{-7} that the cubic ephemeris is an inadequate representation of the rotation of Geminga.

The F test indicates with 97% confidence that the cubic ephemeris with the sinusoidal term given in Table 1 is an appropriate representation of the modulation. Figure 2b shows how the EGRET peaks are visibly narrower with the sinusoidal term included. Of course, it is possible that this sinusoidal term is coincidentally a good representation of timing noise over this 6 yr interval. If the modulation is due to a planet, the RMS residual is the deviation from the sinusoidal fit in Figure 3, 5.6 milliperiod, or 1.3 ms. This is about the same as our phase resolution, so we regard it as an upper limit. The corresponding upper limit on the activity parameter is -1.2 . Examination of Figure II of Cordes (1993) indicates that a value less than -1.2 for Geminga is plausible.

4. Discussion

The absence of annual modulation in Figure 3 demonstrates that the position of Caraveo et al. (1997) is not in error by more than $\sim 0''.5$. And the fact that the timing residuals obtained with Table 1 (even without including the sinusoidal term) are less than 50 milliperiods for all observations strongly suggests that this ephemeris is in fact a coherent solution for the combined *COS-B* and EGRET data. It is now clear why the optimal cubic ephemeris for EGRET alone implies a braking index of 90. The large second derivative is a partial fit to the timing residuals of Figure 3. The extended timing baseline which *COS-B* provides allows a braking index of 90 to be ruled out. We expect that the large second derivative in the *COS-B* data alone is also caused by this effect. The braking index of 17 ± 1 implied by the coherent solution probably reflects timing noise as well. But if it is a long-term property of the pulsar, then it may indicate that Geminga's γ -ray luminosity is decreasing very rapidly as it spins down. Perhaps Geminga is approaching its demise on the outer-gap death line (Chen & Ruderman 1993). Continued timing of Geminga is warranted to distinguish a real braking index from timing noise.

If further timing observations establish the reality of the Geminga planet, it would be the second

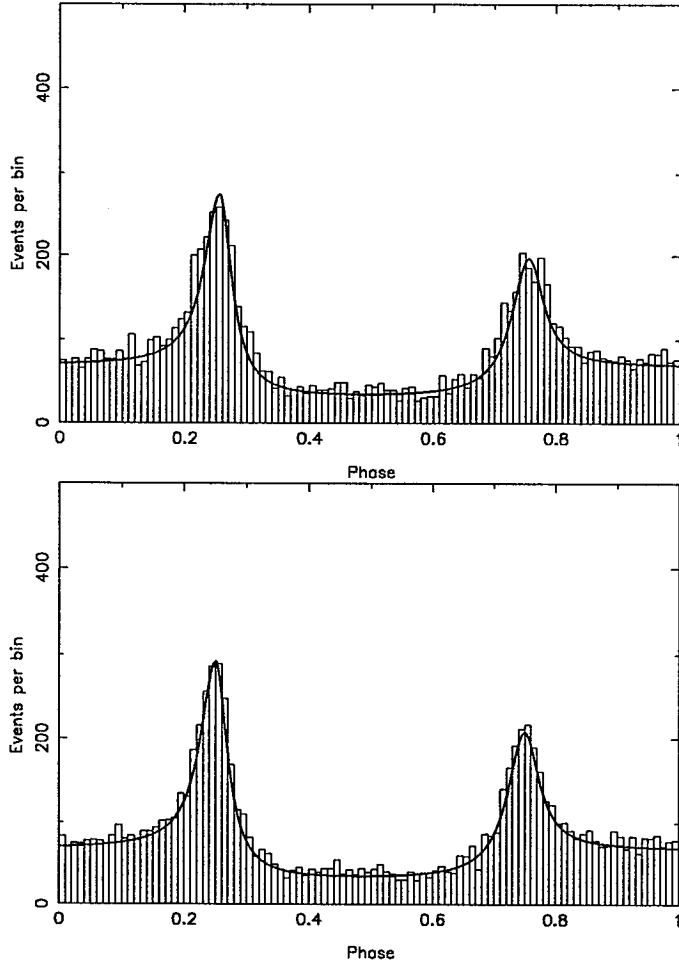


Fig. 2.— The fit of equation 7 for the phase dependence of the Geminga γ -rays is superposed on the histogram of EGRET event phases as determined with the ephemeris of Table 1. A phase offset of 0.194 has been added. (a) The sinusoidal term in Table 1 is not included. The phase obtained with equation 7, $\phi_2 = 0.256$, is used in the fit. (b) The sinusoidal term in Table 1 is included. The phase obtained with equation 7 is $\phi_2 = 0.250$.

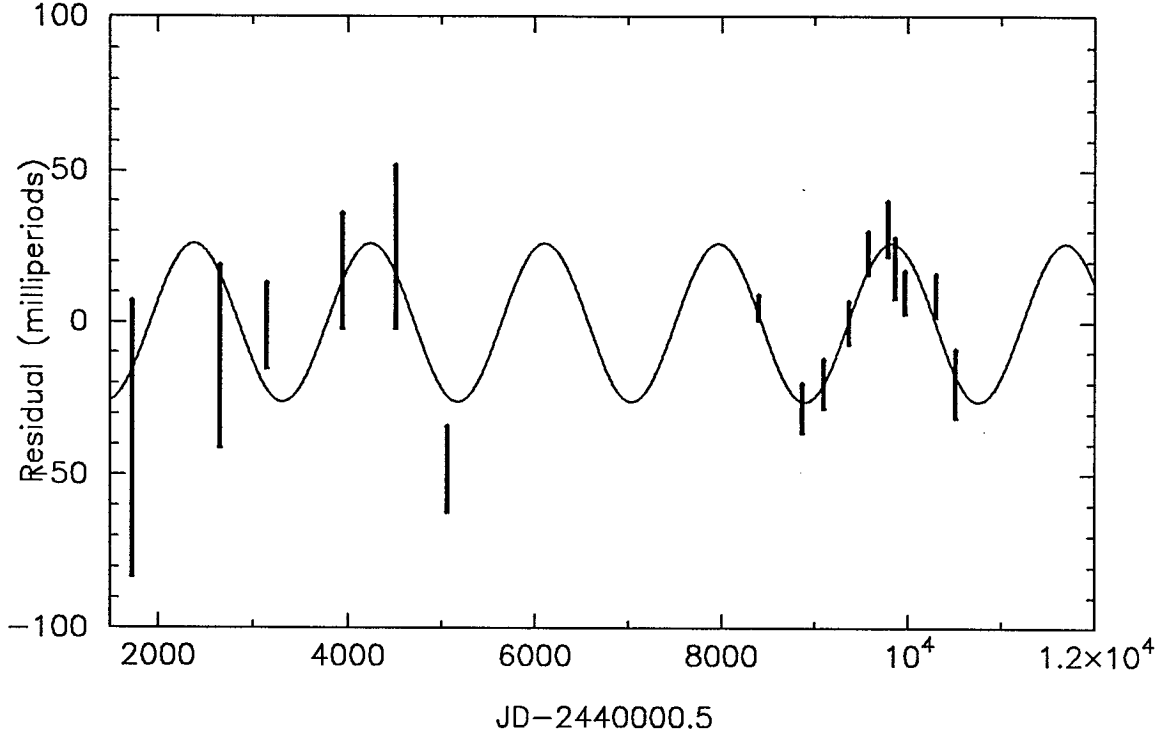


Fig. 3.— The timing residuals for Geminga obtained with the ephemeris of Table 1 without the sinusoidal term are shown with error bars which demarcate the 68% confidence range. The sinusoidal modulation for the planetary parameters in Table 1 is shown. The first residual at JD 2441725 is from the *SAS-2* observation. The residuals from JD 2442651 through JD 2445061 are from *COS-B*. Subsequent residuals are from EGRET observations between 1991.3 and 1997.2.

<p>Epoch, $T_0 = 2446600$ JD (1986 June 18.0 Barycentric Dynamical Time) Frequency at epoch, $f = 4.217705363081(13)$ Hz Frequency derivative, $\dot{f} = -1.9521712(12) \times 10^{-13}$ Hz s$^{-1}$ 2nd frequency derivative, $\ddot{f} = 1.49(3) \times 10^{-25}$ Hz s$^{-2}$ Position at JD 2449794, $\alpha_{2000} = 6^{\text{h}} 33^{\text{m}} 54^{\text{s}}.153$, $\delta_{2000} = +17^{\circ} 46' 12''.91$ Proper motion: 169 mas yr$^{-1}$ at position angle 54° ($\mu_{\alpha_{2000}} = 138$ mas yr$^{-1}$, $\mu_{\delta_{2000}} = 97$ mas yr$^{-1}$)</p> <p>Peak one occurs 0.556(2) of a rotation after T_0.</p>
<p>Possible binary term:</p> <p>Projected semi-major axis, $a_1 \sin i = 6.2(9)$ ms Orbital period, $P_b = 5.1(1)$ yr Epoch of periastron passage, $T_b = \text{JD } 2449360(20)$ Longitude of periastron, $\omega = 90^{\circ}$ Eccentricity, $e = 0.0(4)$</p> <p>Assuming $M_1 = 1.4 M_{\odot}$: $a_2 \sin i = 3.31(4)$ AU $M_2 \sin i = 1.7(2) M_{\oplus}$</p>

Table 1: The “*COS-B*/EGRET 97” ephemeris for GEMINGA obtained through a coherent analysis of *SAS-2*, *COS-B*, and EGRET data. The digit in parenthesis following the derived parameters is the 95% confidence uncertainty of the last digit. See the caption of Figure 1 for a definition of peak one.

confirmed pulsar planet. Two (and perhaps more) planets are known to orbit PSR B1257+12 (Wolszczan 1994). Modulation of timing residuals is seen which may also indicate planets orbiting PSR B1620-26 (Thorsett, Arzoumanian, & Taylor 1993) and PSR B0329+54 (Shabanova 1995). If confirmed, the Geminga planet would be the first confirmed planet around a “slow” pulsar. Such a planet must either survive the SN explosion or be formed from the ejecta of the SN rather than from material accreted from a secondary star as is possible for the planets of ms pulsars such as PSR B1257+12.

If confirmed, the Geminga planet would be the nearest pulsar planetary system. It would be a very interesting system to study in the IR. The planet luminosity at $\lambda = 10\mu\text{m}$ would be $\sim 10^3$ times that of the black-body emission of the pulsar. In principle, spectroscopy could reveal details about the atmosphere which would be of great interest. Unfortunately, the flux density is quite small, 2 nJy or 26 magnitude at $10\mu\text{m}$. If the Geminga planet is confirmed, infra-red spectroscopy will have to be delayed until substantial (but plausible) evolution in observational capability occurs.

We also note in passing that if there is a planet orbiting Geminga and if the inclination of the orbit is within $6''$ of 90° (probability 1×10^{-5}), a total eclipse of Geminga by the planet with a duration of up to 10 minutes will occur once per orbit. In the unlikely event that this alignment exists, the next eclipse will occur within 80 days (95% confidence) of 2000 May 22.

5. Conclusions

We have obtained a cubic ephemeris which describes coherently all γ -ray observations of the rotational phase of Geminga. It appears that Geminga has not glitched during the past 24.2 yr. The derived braking index, 17 ± 1 , may be a manifestation of timing noise. Highly significant timing residuals are apparent that depart from this ephemeris with what could be sinusoidal modulation. With the observations available now, it is not possible to distinguish a planet orbiting Geminga with a period of 5.1 yr from timing noise. Given the wide range of potential timing noise activity for Geminga, neither interpretation implies an unusual activity parameter. We believe that EGRET observations could confirm the timing noise hypothesis in the near future, but that establishing the existence of a planet would take many years, possibly using data of very high quality from the proposed GLAST mission.

If Geminga does not glitch, we expect that the ephemeris we provide in Table 1 will describe its rotation until the year 2008 with a phase error of less than 100 milliperiods. We expect that for most Geminga timing applications, the possible binary term specified in Table 1 will not be important.

J. Mattox acknowledges support from NASA Grants NAG 5-3384 and NAG 5-3806, and J. Halpern from NAG 5-2051. We thank J. Cordes and J. Lazio for running their genetic algorithm on our timing residuals in search of potential planetary solutions. We acknowledge advice from D. Helfand about the ubiquity of timing noise. We also thank D. Thompson for comments and for expediting the delivery of EGRET VP 616.1 data. We also thank J. Cordes, V. Kaspi, and S. Kulkarni for useful discussions.

REFERENCES

- Bennett, K., et al. 1977, A&A 56, 469
 Bertsch, D. L., et al. 1992, Nature 357, 306

- Bignami, G. F., & Caraveo, P. A. 1992, *Nature*, 357, 287
- Bignami, G. F., & Caraveo, P. A. 1996, *ARA&A*, 34, 331
- Bisnovatyi-Kogan, G. S., & Postnov, K. A. 1993, *Nature*, 366, 663
- Caraveo, P. A., Bignami, G. F., Mignani, R., & Taff, L. G. 1996, *ApJ*, 461, L91
- Caraveo, P. A., Lattanzi, M. G., Massone, G., Mignani, R., Makarov, V. V., Perryman, M. A. C., & Bignami, G. F. 1997, *ApJL*, submitted
- Chen, K., & Ruderman, M. 1993, *ApJ*, 402, 264
- Cordes, J. M. 1993, in “Planets Around Pulsars,” ed. J. Phillips, S. Thorsett, & S. Kulkarni, *ASP Conf Ser*, 36, 43
- Fierro, J. M., Michelson, P. F., Nolan, P. L., & Thompson, D. J. 1997, *ApJ*, submitted
- Halpern, J. P., & Holt, S. S. 1992, *Nature* 357, 222
- Halpern, J. P., Martin, C., & Marshall, H. L. 1996, *ApJ*, 473, L37
- Halpern, J. P., & Wang, F. Y.-H., 1997, *ApJ*, 477, 905
- Hermesen, W. et al. 1992, *IAU Circ.*, No. 5541
- Kuzmin, A. D., Losovsky, B. Ya. 1997, *A&A*, submitted
- Lampton, M., Margon, B. & Bowyer, S. 1976, *ApJ*, 208, 177
- Malofeev, V. & Malov, I. F. 1997, *New Astronomy*, submitted
- Mattox, J. R., et al. 1992, *ApJ*, 401, L23
- Mattox, J. R., et al. 1994, *Proc 2nd CGRO Symp*, AIP Conf. Proc. #304, 77
- Mattox, J.R., Halpern, J.P., Caraveo, P.A., 1996, *A&AS*, 120, C77
- Mayer-Hasselwander, H., et al. 1994, *ApJ* 421, 276
- Mignani, R., Caraveo, P. A., & Bignami, G. F. 1994, *Messenger*, 76, 32
- Press, W. H., Teukolsky, S. A., Vetterling, W. T., & Flannery, B. P., 1992, *Numerical Recipes in C* (Cambridge University Press)
- Shabanova, T. 1995, *ApJ*, 453, 779
- Shklovskii, I. S. 1970, *Sov Ast*, 13, 562
- Thompson, D.J., et al. 1977, *ApJ*, 213, 252
- Thorsett, S. E., Arzoumanian, Z., & Taylor, J. H. 1993, *ApJ*, 412, L33
- Wolszczan, A. 1994, *Science*, 264, 538